Title

The reductive half-reaction of xanthine dehydrogenase from Rhodobacter capsulatus: the role of Glu232 in catalysis.

Journal

The Journal of biological chemistry, 289(46)

ISSN

0021-9258

Authors

Hall, James

Reschke, Stefan

Cao, Hongnan

et al.

Publication Date

2014-11-01

DOI

10.1074/jbc.m114.603456

THE JOURNAL OF BIOLOGICAL CHEMISTRY VOL. 289, NO. 46, pp. 32121–32130, November 14, 2014

The Reductive Half-reaction of Xanthine Dehydrogenase from *Rhodobacter capsulatus*

*THE ROLE OF GLU^{232} IN CATALYSIS**

Received for publication, August 6, 2014, and in revised form, September 9, 2014 Published, JBC Papers in Press, September 25, 2014, DOI 10.1074/jbc.M114.603456

James Hall[‡], Stefan Reschke[§], Hongnan Cao[‡1], Silke Leimkühler[§], and Russ Hille[‡2]

From the [‡]Department of Biochemistry, University of California, Riverside, California 92521 and [§]Department of Molecular Enzymology, Institute of Biochemistry and Biology, University Potsdam, 14476 Potsdam, Germany

Background: Kinetic characterization of wild-type xanthine dehydrogenase and variants.
Results: Comparison of the pH dependence of both k_{red} and k_{red}/K_d, as well as k_{cat} and k_{cat}/K_m.
Conclusion: Ionized Glu^{232} of wild-type enzyme plays an important role in catalysis by discriminating against the monoanionic form of xanthine.
Significance: Examining the contributions of Glu^{232} to catalysis is essential for understanding the mechanism of xanthine dehydrogenase.

The kinetic properties of an E232Q variant of the xanthine dehydrogenase from *Rhodobacter capsulatus* have been examined to ascertain whether Glu^{232} in wild-type enzyme is protonated or unprotonated in the course of catalysis at neutral pH. We find that k_{red}, the limiting rate constant for reduction at high [xanthine], is significantly compromised in the variant, a result that is inconsistent with Glu^{232} being neutral in the active site of the wild-type enzyme. A comparison of the pH dependence of both k_{red} and k_{red}/K_d from reductive half-reaction experiments between wild-type and enzyme and the E232Q variant suggests that the ionized Glu^{232} of wild-type enzyme plays an important role in catalysis by discriminating against the monoanionic form of substrate, effectively increasing the pK_a of substrate by two pH units and ensuring that at physiological pH the neutral form of substrate predominates in the Michaelis complex. A kinetic isotope study of the wild-type *R. capsulatus* enzyme indicates that, as previously determined for the bovine and chicken enzymes, product release is principally rate-limiting in catalysis. The disparity in rate constants for the chemical step of the reaction and product release, however, is not as great in the bacterial enzyme as compared with the vertebrate forms. The results indicate that the bacterial and bovine enzymes catalyze the chemical step of the reaction to the same degree and that the faster turnover observed with the bacterial enzyme is due to a faster rate constant for product release than is seen with the vertebrate enzyme.

Molybdenum-containing xanthine oxidoreductases catalyze the sequential oxidative hydroxylation of hypoxanthine to xanthine and xanthine to uric acid in the overwhelming majority of extant organisms. Most of these enzymes are dehydrogenases utilizing NAD^+ as oxidizing substrate, although in mammals the enzyme can be post-translationally modified (by either cysteine oxidation or limited proteolysis) to an oxidase that utilizes O_2 instead (1, 2). The x-ray crystal structures of several of these enzymes are known, including the bovine enzyme in both dehydrogenase and oxidase forms (3) and the dehydrogenase from *Rhodobacter capsulatus* (4). As shown in Fig. 1, the architecture of the active site is highly conserved despite the fact that the vertebrate enzyme is a homodimer with all four redox-active centers (FAD and a pair of [2Fe-2S], in addition to the active site molybdenum center) in a single subunit, whereas the *R. capsulatus* enzyme is an $(\alpha\beta)_2$ tetramer with the FAD and [2Fe-2S] centers in one pair of subunits, and the molybdenum center is a second pair of subunits. Substrate binds between two active site phenylalanine residues (Phe^{914} and Phe^{1009} in the bovine enzyme, Phe^{344} and Phe^{459} in the *R. capsulatus* enzyme), which serve to orient substrate for catalysis. A universally conserved glutamate (Glu^{1261} in the bovine enzyme and Glu^{730} in the bacterial enzyme) is located immediately beneath the molybdenum center and is essential for catalytic activity (5, 6). Other conserved residues in the active site include Glu^{802} and Arg^{880} (Glu^{232} and Arg^{310} in the bacterial enzyme). Given the virtually identical active site structures, the readily expressed recombinant bacterial enzyme constitutes a convenient system to conduct mutational studies (7).

The mechanism of xanthine hydroxylation is now generally understood to proceed as shown in Fig. 2 (8), beginning with proton abstraction from the equatorial Mo-OH by the highly conserved active site glutamate, followed by nucleophilic attack on the sp^2-hybridized carbon of substrate that becomes hydroxylated (C2 in the case of hypoxanthine, C8 in the case of xanthine). Concomitant hydride transfer to the Mo=S group results in reduction of the molybdenum center from Mo^{VI} to Mo^{IV}. The intermediate thus formed has product coordinated to the now reduced molybdenum center via the catalytically introduced hydroxyl oxygen and breaks down by electron transfer out of the molybdenum to the other redox-active cen-

* This work was supported by U.S. Department of Energy Grant DE-FG02-13ER16411 (to R. H.) and by funds from the Deutsche Forschungsgemeinschaft Cluster of Excellence "Unifying Concepts in Catalysis" (to S. L.).
[1] Present address: Dept. of Biochemistry and Cell Biology, Rice University, Houston, TX 77005.
[2] To whom correspondence should be addressed: Dept. of Biochemistry, 1462 Boyce Hall, University of California, Riverside, CA 92521. Tel.: 951-827-6354; Fax: 951-827-2364; E-mail: Russ.Hille@ucr.edu.

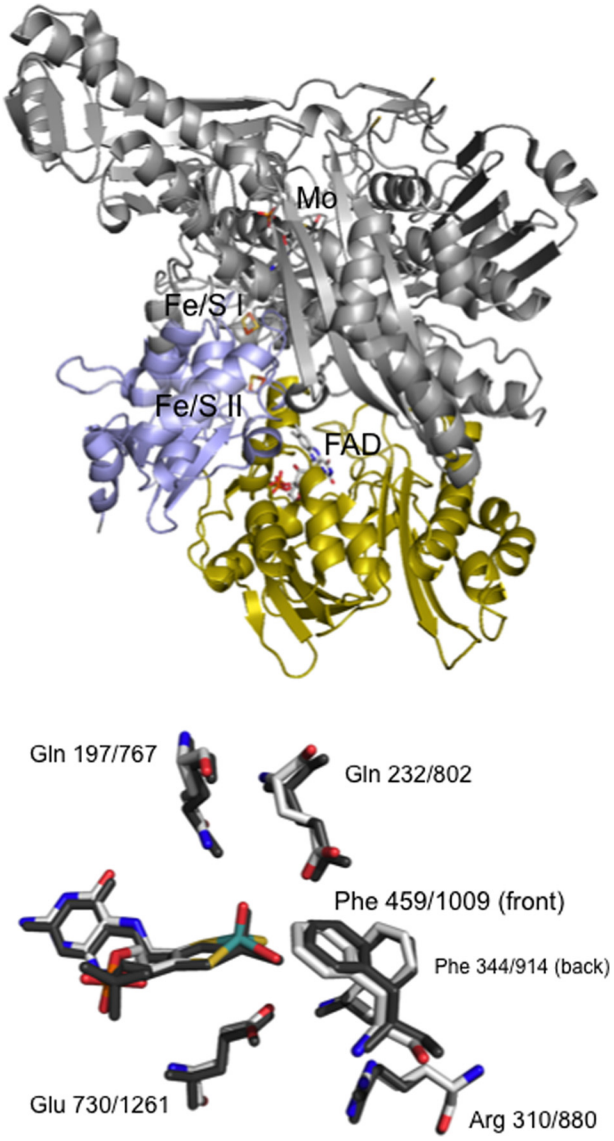

FIGURE 1. **The structure of *R. capsulatus* xanthine dehydrogenase.** *Top panel*, the overall structure of one $\alpha\beta$ protomer of the $(\alpha\beta)_2$ enzyme, with the iron-sulfur- and FAD-binding domains of the small subunit in *blue* and *yellow*, respectively, and the large molybdenum-containing subunit in *gray* (Protein Data Bank code 2W3R). The interface with the other $\alpha\beta$ protomer includes the domain extending out at the *upper left*. The redox-active centers are indicated. *Bottom panel*, a comparison of the active sites of xanthine dehydrogenase from *R. capsulatus* and bovine xanthine oxidase, with the active site of the bacterial xanthine dehydrogenase is shown in *gray* with the numbering of the residues also in *gray*. The bovine xanthine oxidase active site has been overlaid and is shown in a CPK color scheme, whereas the numbering of the residues is in *black*.

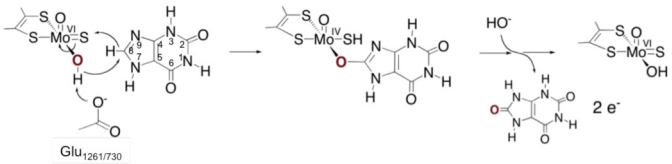

FIGURE 2. **The mechanism of the reductive half-reaction of xanthine oxidase.**

ters of the enzyme and displacement of product from the molybdenum coordination sphere by hydroxide from solvent. Depending on reaction conditions and substrate, the latter sequence of events can give rise to a Mo(V) species containing product coordinated to the molybdenum center that gives rise to the long-studied "very rapid" EPR signal (9, 10), although with most substrates and under most reaction conditions, this is a minor pathway that contributes no more than ~10% of the total catalytic throughput. It is notweworthy, however, that formation of the very rapid Mo(V) species is thus an oxidative event, arising from the loss of an electron from a precursor Mo(IV) species that is EPR-silent.

Previous mutagenesis studies of the recombinant *R. capsulatus* enzyme have involved substitution of Glu^{730} and Glu^{232} to Ala (6), and Arg^{310} to Met (11) (equivalent to Glu^{1261}, Glu^{802}, and Arg^{880}, respectively, in the bovine enzyme). Mutation of Glu^{730} to Ala abolishes all activity toward xanthine in rapid reaction kinetic studies at neutral pH, with a minimum reduction in k_{red} (and, correspondingly, the steady-state k_{cat}) of 10^7, consistent with the role of this residue as a general base, abstracting the Mo-OH proton to initiate catalysis (6). Mutation of Arg^{310} to Met also results in a large reduction in k_{red}, by a factor of 10^4, an effect attributed to $Arg^{310/880}$ stabilizing negative charge on the heterocycle in the course of nucleophilic attack (11). The E232A variant exhibited a more modest 12-fold decrease in k_{red} and a 12-fold increase in K_d in the reductive half-reaction, relative to wild-type enzyme, comparable with the effect seen on the steady-state kinetic behavior of an E803V variant of the human enzyme (13). Given the effect of the mutation on both K_d and k_{red}, it is evident that Glu^{232} is involved with both substrate binding and transition state stabilization, although its specific role has been somewhat controversial. Computational studies have suggested that $Glu^{232/802}$ is ionized and plays a role in facilitating proton tautomerization between N3 and N9 of xanthine in the course of catalysis (6, 14–16). Such a role is consistent with the orientation of xanthine observed in complexes of the inactive, desulfo forms of both the bovine and *R. capsulatus* enzymes (Fig. 3*A*), where $Glu^{802/232}$ appears to be deprotonated and serving as a hydrogen-bonding acceptor to the protonated N3 of substrate (17, 18). On the other hand, in the structure of xanthine oxidase with the slow substrate FYX-051 (19) Glu^{802} appears to be protonated, serving as a hydrogen-bonding donor to an aromatic nitrogen of the substrate. Glu^{802} also appears to be protonated in crystal structures of the rat enzyme in complex with urate (20), again appearing to serve as a hydrogen-bonding donor, this time to N7 of urate, which is seen in an inverted orientation relative to that observed with xanthine (Fig. 3*B*). Quantum mechanics/molecular mechanics studies have also been performed on xanthine oxidase, in which it is presumed that Glu^{802} is protonated at the outset of catalysis (21).

The above mutational effects are predicated on the assumption that the chemical step of the reaction is rate-limiting in the variants. It is known, however, that at least with the wild-type bovine enzyme, product release is in fact rate-limiting. To further evaluate the role of Glu^{232} in catalysis, kinetic studies on the reductive half-reaction of a nonionizing E232Q variant of the recombinant *R. capsulatus* enzyme have been conducted. We find that the E232Q variant exhibits the same 12-fold decrease in k_{red} as the E232A variant, a result that is inconsistent with the argument that a neutral (protonated) $Glu^{802/232}$ acts as a hydrogen-bonding donor to the substrate during catal-

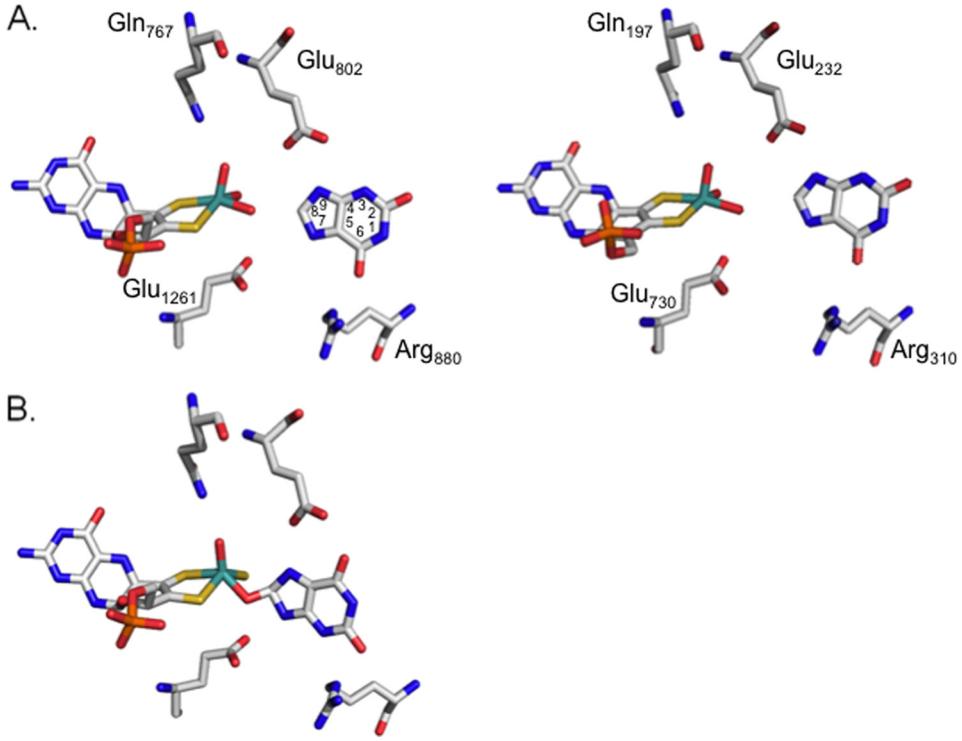

FIGURE 3. **Crystal structures of xanthine oxidase with substrate.** *A* and *B*, the x-ray crystal structures of desulfo bovine xanthine oxidase (*A*, *left*; Protein Data Bank code 3EUB) and *R. capsulatus* xanthine xanthine dehydrogenase (Protein Data Bank with xanthine bound (Protein Data Bank code 2W3S), where an ionized glutamate 802/232 acts as a hydrogen bonding acceptor from the substrate N3 nitrogen and reduced bovine xanthine oxidase (*B*) with urate bound (Protein Data Bank code 3AMZ), with neutral glutamate 802 acting as a hydrogen-bonding donor to the N9 of urate.

ysis. The pH dependence of the reductive half-reaction has also been determined that, when compared with the behavior of the wild-type enzyme, suggests a role for Glu^{232} in discriminating against the monoanionic form of substrate. We have also undertaken a kinetic isotope effect study to evaluate the extent to which the chemical step of the reaction is rate-limiting in the case of the wild-type *R. capsulatus* enzyme and found that its considerably faster turnover relative to the bovine enzyme is due to significantly faster product release, the chemical step of the reaction for the two enzymes occurring at comparable rates.

EXPERIMENTAL PROCEDURES

Enzyme Purification, Metal, and Cofactor Content Quantification—Recombinant *R. capsulatus* xanthine dehydrogenase was heterologously expressed in *Escherichia coli* TP 1000 cells and purified as described previously (7), by nickel-nitrilotriacetic acid chromatography, Q-Sepharose, and size exclusion chromatography. E232Q was mutated to glutamine in the enzyme by PCR mutagenesis, as described previously (18). Metal content analysis was performed using an Optima 2100DV inductively coupled plasma-optical emission (ICP-OES)[3] spectrometer (PerkinElmer Life Sciences). Protein samples were incubated overnight in a 1:1 mixture with 65% nitric acid (Suprapur; Merck) at 100 °C. Protein samples were diluted with a 10-fold volume of ultrapure water (Millipore) prior to ICP-OES analysis. The multielement standard solution XVI (Merck) was used as a reference (22).

Enzyme Assay Methods—UV-visible absorption spectra were obtained, and steady-state experiments were performed using a Hewlett-Packard 8452 diode array spectrophotometer. To follow the fractional conversion of xanthine to uric acid by xanthine oxidase, substrate and enzyme were added to 1 ml of air equilibrated buffer (0.1 M sodium pyrophosphate, 0.3 mM EDTA, pH 8.5). The formation of uric acid was monitored at 295 nm ($\Delta\epsilon_{295\ nm} = 9600\ M^{-1}\ cm^{-1}$). For bacterial XDH1, xanthine, NAD^+, and enzyme were subsequently added to 1 ml of air-equilibrated buffer (50 mM potassium phosphate, 0.1 mM EDTA, pH 7.9). The formation of NADH ($\Delta\epsilon_{340\ nm} = 6200\ M^{-1}\ cm^{-1}$) was monitored in addition to the formation of uric acid.

The pH-dependent steady-state kinetics where carried out at 25 °C in 1-ml cuvettes in 100 mM CAPS, 100 mM KCl (pH 9–10), 50 mM Tris, 100 mM NaCl (pH 7–9), and 100 mM MES, 100 mM KCl (pH 5.5–6.5) using 500 μM NAD and different xanthine concentrations (25, 50, 75, 100, and 200 μM). The reaction was followed by 1 min at 340 nm with a Shimadzu UV-2401PC UV-visible recording spectrophotometer. Enzyme concentration was 0.675 mg/ml for wild type and 6.75 mg/ml for E232Q.

Rapid Reaction Kinetics—The reductive half-reaction kinetics were performed using an Applied Photophysics, Inc. SX-18MV stopped flow spectrophotometer. Enzyme was made anaerobic in glass tonometers by evacuating and flushing with oxygen scrubbed argon gas (obtained from Airgas) for between 30 and 60 min. Substrate solutions were made anaerobic by bubbling solutions in glass syringes for 15–30 min. Standard

[3] The abbreviations used are: ICP-OES, inductively coupled plasma-optical emission spectrometer; XDH, xanthine dehydrogenase; CAPS, 3-(cyclohexylamino)propanesulfonic acid; CHES, 2-(cyclohexylamino)ethanesulfonic acid.

buffer conditions for xanthine oxidase were 100 mM sodium pyrophosphate, 0.3 mM EDTA, pH 8.5, at 25°C. Reactions were observed at 450 nm, monitoring the disappearance of absorbance because of reduction. For bacterial xanthine dehydrogenase, standard buffer conditions were 50 mM potassium phosphate, 0.1 mM EDTA, pH 7.8. Reactions involving the bacterial xanthine dehydrogenase were monitored at 465 nm. The reaction mixtures after mixing typically had 5–10 μM enzyme and varying concentrations of substrate. The reaction with each substrate concentration used was repeated in triplicate. The kinetic transients were fit to single exponentials to obtain rate constants, which were averaged for each substrate concentration. Each k_{obs} was then plotted against substrate concentration, and the hyperbolic curve fit using SigmaPlot to obtain values for k_{red} and the dissociation constant, K_d. pH dependence studies on the reductive half-reaction were conducted between pH units of 6–11 using conditions previously reported by Kim *et al.* (23). Buffers at the various pH units included 0.1 M MES (pH 6.0), 0.1 M MOPS (pH 7.0), 0.1 M Tris-HCl (pH 8.0), 0.1 M CHES (pH 9.0, 9.5), 0.1 M CAPS (pH 10, 10.5, 11.0), each also supplemented with 0.3 mM EDTA and 0.1 M KCl. For both the steady-state and rapid reaction data, pH profiles for a given kinetic parameter L were fit to the following equation for a double-ionization mechanism, with the maximum theoretical value for L, L_{max}, and the two pK_a values pK_1 and pK_2 as floating variables.

$$L_{obs} = L_{max}/[1 + ([H^+/10^{(-pKa1)}) + (10^{(-pKa2)}/[H^+]) \quad \text{(Eq. 1)}$$

Kinetic Isotope Effect Studies—The deuterium isotope effect on the steady-state kinetics of the *R. capsulatus* xanthine dehydrogenase was analyzed in the conventional manner in solutions. Typical experiments involved addition of catalytic amounts of enzyme to 2.5 ml of buffer solution at pH/D 7.8 containing 50 mM potassium phosphate, 0.1 mM EDTA, and 500 μM NAD^+ as the terminal electron acceptor. The solutions were made anaerobic by bubbling argon gas through it for 20 min in a sealed quartz cuvette. The buffer solution, including NAD^+, was preincubated at 25 °C followed by the addition of first xanthine and then enzyme. Changes in absorbance change at 295 nm were monitored. The initial reaction mix contained a fixed concentration of functional *R. capsulatus* xanthine dehydrogenase (~2 nM functional active sites) and varying concentrations of substrates (5–200 μM). The initial rates were calculated from linear fits of the first 20–120 s of each transient. Xanthine oxidase assays used 5 nM functionally active sites and were measured in air equilibrated 0.1 M sodium pyrophosphate, pH 8.5, that did not contain NAD^+.

Competition experiments were used to determine the tritium isotope effect on (V/K) were performed following a slight modification of the method described by D'Ardenne and Edmondson (24). Catalytic amounts of enzyme (5 nM functional active sites for xanthine oxidase and 2 nM functional active sites for bacterial XDH) were incubated at room temperature with xanthine concentrations of 40 μM for bovine xanthine oxidase and 200 μM xanthine for bacterial XDH. Air-saturated buffers were used for xanthine oxidase, whereas anaerobic solutions of 500 μM NAD^+ were used for the bacterial XDH samples. Levels of radiolabeled [8-^{3}H]xanthine in each sample were ~0.1 μCi/ml. Fractional conversion of xanthine to uric acid was determined via UV-visible spectroscopy, monitoring the reaction to completion and determining the point at which 10–20% of the total absorbance change at 295 nm was reached. Once 10–20% fractional conversion was reached, the reaction mixture was quenched by the addition of 10% (w/v) trichloroacetic acid. Substrate ([8-^{3}H]xanthine) and product (^{3}H-labeled water) were separated by HPLC (Supelco C18 column, isocratic conditions, 1 ml/min, 50 mM sodium phosphate, pH 6.0) with tritiated water eluting at ~3 min and [8-^{3}H]xanthine eluting at ~10 min.

Competitive (V/K) isotope effects were calculated from quantitation of the radioactivity in the tritiated water and the [8-^{3}H]xanthine using the following equation (24, 25),

$$\frac{(V/K)_H}{(V/K)_T} = \frac{\ln(1-f)}{\ln[(1-f)R_t^p/R_s^0]} \quad \text{(Eq. 2)}$$

where f is the fractional conversion of substrate to products, R_p^t is the ^{3}H ratio of products at time t, and R_s^0 is the ^{3}H ratio of the substrate at $t = 0$. The ratio at 0% conversion was monitored to correct for the naturally occurring ^{3}H exchange with water in the absence of enzyme.

Knowing $^{H/D}(V/K)$ and $^{H/T}(V/K)$, the intrinsic isotope effect was calculated using Equation 3 (26),

$$\frac{^{H/D}(V/K) - 1}{^{H/T}(V/K) - 1} = \frac{^{D}k - 1}{^{D}k^{1.442} - 1} \quad \text{(Eq. 3)}$$

with both the primary deuterium isotope effect ($^{H/D}V$) and the intrinsic isotope effect (^Dk) thus known, the f_v or fractional velocity of the chemical step in relation to the overall rate of the reaction was calculated using Equation 4 (24),

$$f_V = (^{H/D}V - 1)/(^{D}k - 1) \quad \text{(Eq. 4)}$$

where f_v represents the fractional extent to which the chemical step of the reaction ($k_{C\text{-}H}$) contributes to the overall k_{cat}; $1/f_v$ thus gives how much faster the chemical step of the reaction is than k_{cat}, thus multiplying the inverse of f_v by the value for k_{cat} gives the approximate rate of the chemical step. The estimated values for the rate of product dissociation (k_{off}) was calculated using Equation 5.

$$\frac{1}{k_{cat}} = \frac{1}{k_{C\text{-}H}} + \frac{1}{k_{off}} \quad \text{(Eq. 5)}$$

RESULTS AND DISCUSSION

Steady-state Kinetics of the E232Q Variant of R. capsulatus Xanthine Dehydrogenase—Structural studies with both the bovine and *R. capsulatus* enzymes indicate that Glu^{802} (equivalent to Glu^{232} in the *R. capsulatus* enzyme) is within hydrogen-bonding distance of substrate and could act as either a hydrogen bonding acceptor (in its ionized state) to substrate N3 or hydrogen-bonding donor (in the neutral form, although this would require a pK_a above 8, well outside the normal range for glutamates) to the C_6=O carbonyl (Fig. 3) (17, 18). Past studies by Leimkühler *et al.* have demonstrated a 12-fold decrease of E232A variant in k_{red} compared with the wild-type enzyme (6).

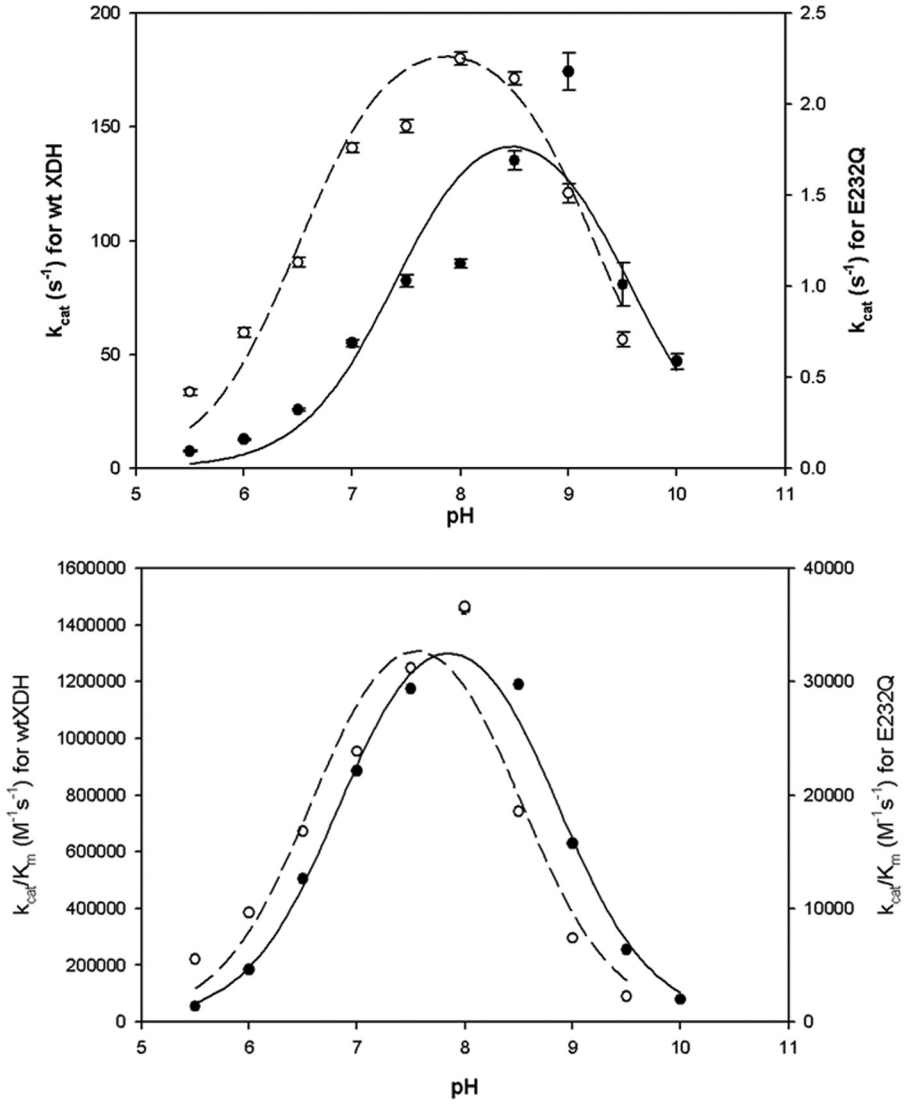

FIGURE 4. **pH dependence of k_{cat} and k_{cat}/K_m for wild-type *R. capsulatus* xanthine dehydrogenase (*closed circles*) and the E232Q variant (*open circles*).** Assays were conducted at 25 °C in 1-ml cuvettes in 100 mM CAPS, 100 mM KCl (pH 9–10), 50 mM Tris, 100 mM NaCl (pH 7–9), NAD^+ and varying concentrations of xanthine (25, 50, 75, 100, 200, and 500 μM). The reaction was followed for 1 min at 340 nm with a Shimadzu UV-2401PC UV-visible recording spectrophotometer. The k_{cat} values were corrected for the molybdenum content of the protein sample as determined by ICP-OES. For k_{cat}, the pK_a values defining the pH profile for wild-type enzyme were 7.4 and 9.6, and for the E232Q variant they were 6.5 and 9.2. For k_{cat}/K_m, the pK_a values were 6.8 and 8.8 for wild-type enzyme and 6.6 and 8.5 for the E232Q variant.

Although the alanine variant assesses the effect of removing the carboxylate side chain of glutamate, it does not provide specific insight its ionization state. We have thus prepared an E232Q variant of the *R. capsulatus* xanthine dehydrogenase variant and examined its kinetic behavior in detail. If, as has been suggested (19), Glu^{232} is neutral and acts as a hydrogen-bonding donor during catalysis, then the E232Q variant should still be able to hydrogen bond with the substrate, and there should be little change in activity. If, on the other hand, Glu^{232} is ionized, a decrease in activity with the E232Q variant is expected, at least as much as the 12-fold decrease in k_{red} seen previously with the E232A mutant (6).

The pH dependence the steady-state values k_{cat} and k_{cat}/K_m for wild-type xanthine dehydrogenase and the E232Q variant are shown in Fig. 4. For both enzyme forms, each kinetic parameter exhibits bell-shaped pH dependence. For wild-type enzyme, the pK_a values that define the pH profile for k_{cat} are 7.4 and 9.6; for the E232Q variant, these values decrease to 6.5 and 9.2. The maximum of k_{cat} for the wild-type enzyme is $\sim$150 s^{-1}, which decreases with the E232Q variant to 3.3 s^{-1} (Table 1). For k_{cat}/K_m, the pK_a values for wild-type enzyme are 6.8 and 8.8, which are lowered only very modestly in the E232Q variant to 6.6 and 8.5. The pK_a values for k_{cat}/K_m with wild-type enzyme determined here are in fair agreement with the values of 6.3 and 7.7 reported previously by Aguey-Zinsou *et al.* (27), who monitored catalysis electrochemically (the pH dependence of k_{cat} was not reported in this work). However, here the autocatalytic reaction with uric acid was measured directly at the electrode, which might explain the difference in the pH profile, because the latter is rather related to the ionization of uric acid (28). The maximal theoretical value for k_{cat}/K_m, obtained from the fit to the pH profile as described under "Experimental Procedures," decreases from 2.0×10^6 M^{-1} s^{-1} with the wild-type enzyme to 6×10^4 M^{-1} s^{-1} for the E232Q variant.

TABLE 1

Values of k_{cat}, K_m, and k_{cat}/K_m for wild-type *R. capsulatus* xanthine dehydrogenase and the E232Q variant

The values are the results of steady-state kinetic measurement of fresh purified protein. The k_{cat} values were corrected by molybdenum saturation as determined by ICP-OES.

	R. capsulatus XDH					
	Wild-type			E232Q		
pH	k_{cat}	K_m	k_{cat}/K_m	k_{cat}	K_m	k_{cat}/K_m
	s^{-1}	μM	$\times 10^6\ M^{-1}\ s^{-1}$	s^{-1}	μM	$\times 10^6\ M^{-1}\ s^{-1}$
5.5	7. 52 ± 0.41	138 ± 17.5	0.0544	0.418 ± 0.016	76.1 ± 8.07	0.0055
6.0	12.6 ± 0.27	68.3 ± 4.20	0.184	0.744 ± 0.025	77.2 ± 7.30	0.0096
6.5	25.6 ± 0.69	50.7 ± 4.39	0.505	1.13 ± 0.025	67.2 ± 4.26	0.0168
7.0	54.9 ± 1.46	61.7 ± 4.94	0.885	1.76 ± 0.027	73.8 ± 3.19	0.0239
7.5	82.3 ± 2.77	70.0 ± 6.73	1.18	1.88 ± 0.035	60.3 ± 3.40	0.0311
8.0	89.8 ± 2.07	61.8 ± 4.25	1.45	2.25 ± 0.034	61.4 ± 2.80	0.0366
8.5	135 ± 4.21	114 ± 8.67	1.19	2.14 ± 0.035	115 ± 4.53	0.0186
9.0	174 ± 8.15	277 ± 24.8	0.629	1.51 ± 0.054	205 ± 15.3	0.0074
9.5	80.7 ± 9.37	318 ± 68.1	0.254	0.706 ± 0.040	316 ± 33.1	0.0022
10.0	46.9 ± 3.47	594 ± 68.4	0.0790			

TABLE 2

Kinetic parameters for the reductive half-reactions of wild-type *R. capsulatus* xanthine dehydrogenase and the E232Q variant

	R. capsulatus XDH					
	Wild-type			E232Q		
pH	k_{red}	K_d	k_{red}/K_d	k_{red}	K_d	k_{red}/K_d
	s^{-1}	μM	$\times 10^6\ M^{-1}\ s^{-1}$	s^{-1}	μM	$\times 10^6\ M^{-1}\ s^{-1}$
6.0				8.3 ± 0.46	104 ± 15	0.080
7.0	65 ± 6	34 ± 14	1.9	18.3 ± 2.1	108 ± 32	0.17
7.8	217 ± 8	42 ± 6	5.16	17.3 ± 1.9	124 ± 33	0.14
8.5				12.6 ± 1.3	106 ± 31	0.12
9.0	239 ± 8	340 ± 25	0.70	5.12 ± 0.23	234 ± 22	0.022
10.0	140 ± 4	1458 ± 95	0.096	0.340 ± 0.044	ND[a]	

[a] ND, not determined.

TABLE 3

Kinetic parameters for the reductive half-reaction of *R. capsulatus* xanthine dehydrogenase and variants with xanthine at pH 7.8 at 25 °C

Enzyme	k_{red}	K_d	k_{red}/K_d
	s^{-1}	μM	$\mu M^{-1}\ s^{-1}$
Wild-type	217 ± 13	42.1 ± 10.0	5.15
E232Q	17 ± 1.9	124 ± 33	0.14

The Reductive Half-reaction of the E232Q Variant with Xanthine—We next examined the reductive half-reaction kinetics of the E232Q variant with xanthine, with the results summarized in Tables 2 and 3. As shown in Fig. 5*A*, at pH 7.8, 25°C, the kinetics of reduction of both wild-type xanthine dehydrogenase and the E232Q variant by xanthine exhibit hyperbolic dependence on xanthine concentration. The limiting rate of reduction, k_{red}, for the wild-type enzyme with xanthine was found to be 217 ± 13 s^{-1}, and the apparent dissociation constant, K_d, was found to be 42.1 ± 10.0 μM, in good agreement with previously published results (k_{red} = 67.3 s^{-1}, K_d = 33.6 μM) (7) after taking into account the lower temperature in the earlier work, 4 °C. The E232Q variant exhibits a 12-fold decrease in k_{red} and a ~3-fold increase in K_d compared with wild type. These values can be compared with the published results seen with the E232A variant, which exhibited a 12-fold decrease in k_{red} and 12-fold increase in K_d compared with wild type. It is evident that both variants compromise k_{red} to the same degree, although the effect on K_d is somewhat more modest in the E232Q variant than in the E232A variant. Nevertheless, the comparable effects of the two mutations on k_{red} are consistent with the interpretation that $Glu^{802/232}$ is in fact deprotonated in the course of catalysis (6, 14–16). Both the magnitude of k_{red} seen with the E232Q variant and its pH dependence is consistent with the behavior of the steady-state k_{cat}, as expected given that the overall rate-limiting step in catalysis is known to reside in the reductive half-reaction (24).

The pH Dependence of Wild-type R. capsulatus Xanthine Dehydrogenase and the E232Q Variant—Previous pH dependence studies of bovine xanthine oxidase with xanthine as substrate (23, 29) have yielded a sigmoidal curve (ascending at higher pH) for the rapid reaction kinetic parameter k_{red} (which tracks the breakdown of the E·S complex) with a pK_a of 7.5. This is the sole ionization that is clearly defined between pH 6 and 10, indicating that no other active site residue ionizes in a catalytically critical way in this pH range. (Although there is evidence of decrease at very high pH, it is not sufficiently well defined as to assign a specific pK_a.) For k_{red}/K_d (which tracks the reaction of free enzyme with free substrate in the low [substrate] regime and which will respond to ionizations of free enzyme as well as free substrate), on the other hand, a bell-shaped curve is clearly observed. Fits using Equation 6,

$$k_{cat}/K_m = (k_{cat}/K_m)_{max}/(1 + 10^{pKa1\ -\ pH} + 10^{pH\ -\ pKa2}) \quad \text{(Eq. 6)}$$

yield pK_a values of 6.6 and 7.4 for the ascending and descending limbs of the plot, respectively. The latter ionization agrees well with the known pK_a for xanthine of 7.6 (31), and the former has been assigned to Glu^{1261} acting as an active site base (32). The implication is that enzyme binds to and acts on the neutral rather than monoanionic form of the substrate (consistent with a reaction mechanism predicated on nucleophilic attack on substrate).

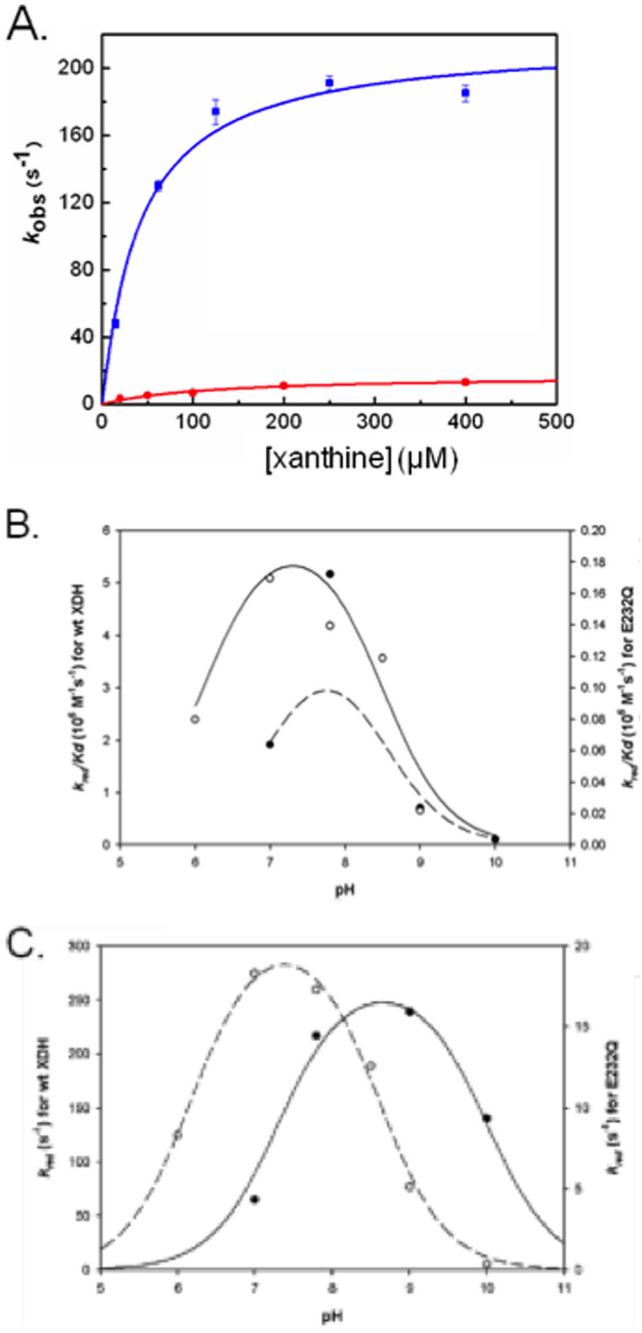

FIGURE 5. *A*, plots of observed rate constant k_{obs} *versus* [substrate] for the anaerobic reductive half-reaction of wild-type (*blue*) and E232Q (*red*) enzyme. All reactions were carried out under anaerobic conditions in 50 mM potassium phosphate, 0.1 mM EDTA, pH 7.8, at 25 °C, following reduction of enzyme by excess xanthine was followed at 465 nm. Hyperbolic fits to the data (*solid lines*) yielded $k_{red} = 217\ s^{-1}$ and K_d 432 μM for wild-type enzyme and 17 s^{-1} and 124 μM for the E232Q variant. *B*, the pH dependence of k_{red}/K_d for wild-type xanthine dehydroganase (*black circles*) and the E232Q variant (*white circles*) with xanthine. The fit for the pH dependence of k_{red}/K_d for the wild-type enzyme gave pK_a values of ~7 and ~8.5 and a theoretical maximum value of $\sim 4 \times 10^6\ M^{-1}\ s^{-1}$. The fit for the pH dependence of k_{red}/K_d for XDH E232Q variant gave pK_a values of 6.1 and 8.5 and a theoretical maximum value of $0.20 \times 10^6\ M^{-1}\ s^{-1}$. It is to be noted that because of the two pK_a values for k_{red}/K_d for wild-type bacterial XDH being close to each other, the theoretical maximum is significantly underestimated. *C*, the pH dependence of k_{red} for wild-type xanthine dehydrogenase (*black circles*) and the E232Q variant (*white circles*) with xanthine. The fit for the pH dependence of k_{red} for wild-type bacterial XDH gave pK_a values of ~7.3 and ~10 and a theoretical maximum value of ~270 s^{-1}. The fit for the pH dependence of k_{red} for XDH E232Q variant gave pK_a values of 6.18 and 8.59 and a theoretical maximum value of 21.2 s^{-1}.

In examining the pH dependence of the reductive half-reaction of the bacterial enzyme (summarized in Table 2), we find that k_{red}/K_d for the wild-type enzyme is also bell-shaped, consistent with the rate-limiting step being in the reductive half-reaction of the overall catalytic sequence (as is the case with the bovine enzyme). The pH dependence on k_{red}/K_d also exhibits bell-shaped curve with pK_a values of ~7 and 8.5 (Fig. 5*B*). By contrast to the bovine enzyme, however, we find that the pH dependence of k_{red} with the wild-type bacterial enzyme is also clearly bell-shaped curve, yielding pK_a values of 7.3 and 10 for the ascending and descending limbs, respectively, and a theoretical maximum value for k_{red} of ~270 s^{-1} (Fig. 5*C*). The somewhat different pH dependence of k_{red} seen with the bovine and bacterial enzymes, with a clear descending limb in the pH profile at high pH only observed with the bacterial enzyme, suggests that although both enzymes preferentially bind the neutral form of substrate—that is, shift its pK_a to a higher value—the bovine enzyme does so to a somewhat greater degree than the bacterial form. Still, the shift in pK_a for xanthine on binding the bacterial enzyme is increased 2.5 pH units over that in free solution (as compared to the bovine enzyme, where the shift is at least 3.5 pH units).

With the E232Q variant, the pH dependence on k_{red}/K_d also exhibits bell-shaped curve with pK_a values of 6.1 and 8.6 (Fig. 5*C*), generally consistent with the results seen with wild-type enzyme taking into account the significantly lower maximal value seen with the variant ($2.0 \times 10^5\ M^{-1}\ s^{-1}$ as compared with $\sim 4 \times 10^6\ M^{-1}\ s^{-1}$). As shown in Fig. 5*C*, the pH profile for k_{red} is also bell-shaped (as seen with the wild-type bacterial enzyme), but the maximal value is 21 s^{-1}, significantly lower than the value of 270 s^{-1} seen with the wild-type enzyme. The pK_a values for the pH dependence of k_{red} with the E232Q variant are 6.3 and 8.6, comparable with the values seen in the pH dependence of k_{red}/K_d with the E232Q variant (Fig. 5*C*). The significant reduction in the maximal value for k_{red} upon substitution of glutamine for glutamate, comparable with that seen previously with the E232A variant (6), clearly indicates that negative charge and not hydrogen bond donating capacity is the catalytically essential feature of this residue. Our interpretation of the difference in pK_a values for k_{red} with wild-type and E232Q variant is that the variant does not shift the pK_a of substrate to nearly the same extent as does wild-type enzyme, with the result that the monoanion of xanthine is able to bind in the active site. Deprotonation of xanthine typically occurs at N3 (15, 31), so based upon the orientation of xanthine in the crystal structures of the wild-type enzymes shown in Fig. 3 (17), the negative charge of $Glu^{802/232}$ would repel xanthine exhibiting a negative charge delocalized over N3 and the C2 oxygen (Fig. 6, *A* and *B*). Substitution of Glu^{232} to Gln abolishes this electrostatic repulsion (Fig. 6, *C* and *D*), and the neutral but polar glutamine would also be able to interact favorably with both the neutral and monoanionic forms of substrate (although only the former would be catalytically effective, because of the significantly lower susceptibility of the negatively charged monoanion to nucleophilic attack).

We note that substrate orientation in the active site is likely to depend critically on its ionization state. The negative charge at N3 of the monoanion could well be stabilized by the posi-

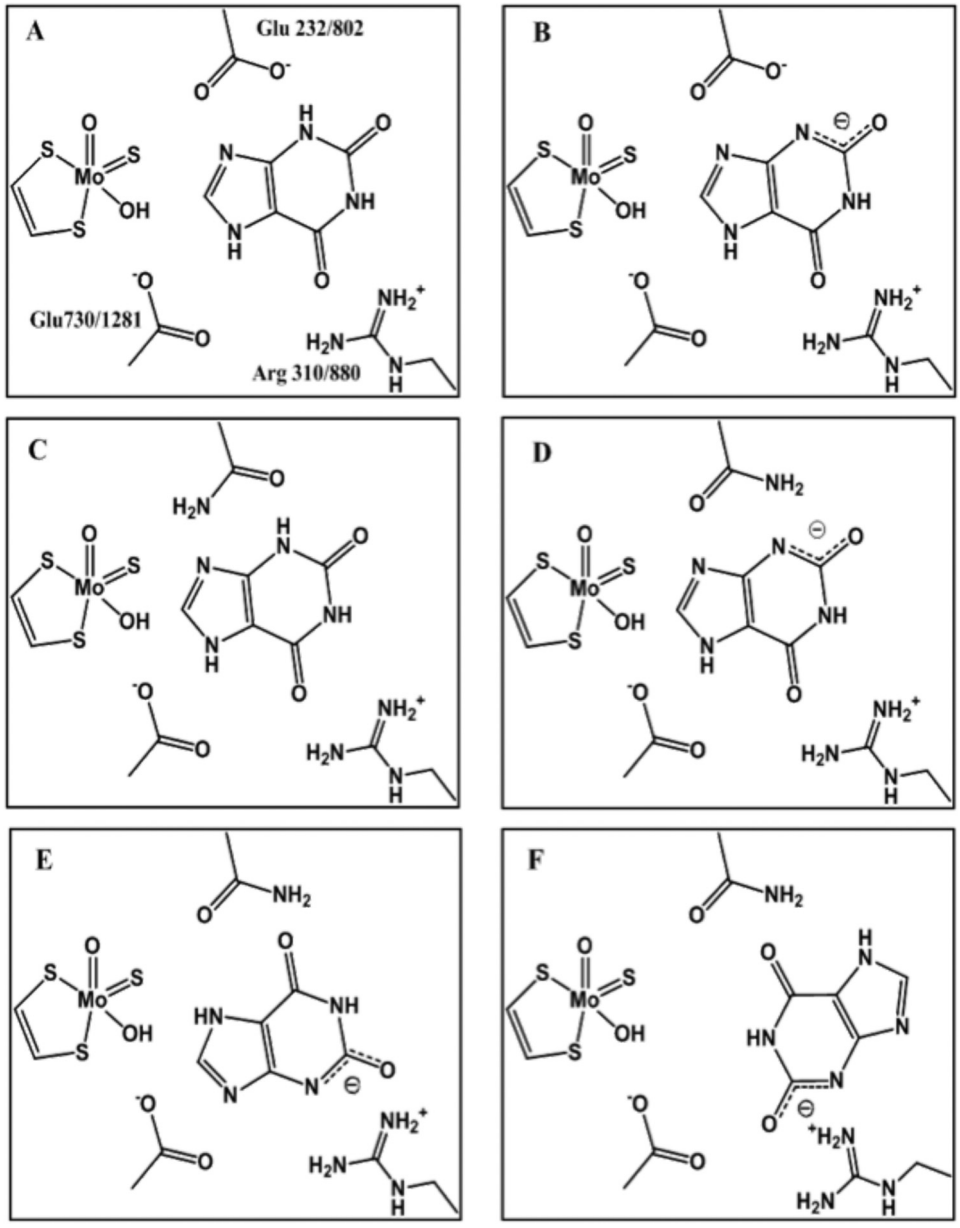

FIGURE 6. **Proposed orientations of xanthine binding in the active site of xanthine oxidoreductase, using the predominant tautomers of the neutral and monoanionic forms of xanthine (31).** *A*, the "right side up" orientation of neutral xanthine bound in the active site, as seen crystallographically (17, 18). *B*, a model of a right side up orientation of the monoanionic form of xanthine bound in the active site, an unlikely orientation given the proximity of negative charges on enzyme and substrate. *C*, a proposed right side up orientation of neutral xanthine bound in the active site of the E232Q variant. *D*, a proposed right side up orientation for the monoionic form of xanthine bound to the E232Q variant. *E* and *F*, proposed upside down orientation of the monoionic form of xanthine with the E232Q variant.

tively charged Arg^{310}, resulting in inversion of substrate in the active site that would allow Gln^{232} in the variant bacterial enzyme could hydrogen bond to the C6 carbonyl group in either of two ways (Fig. 6, *E* and *F*). In the wild-type enzyme, the negative charge on Glu^{232} driving substrate protonation, this binding mode would be unlikely under physiological conditions. We reiterate, however, that an inverted orientation has been observed crystallographically for reduced bovine xanthine oxidoreductase in complex with urate (20), as shown in Fig. 3*B* and corresponding to the orientation shown in Fig. 6*E*. At neutral pH, urate (which has a first pK_a of 5.8 (33)) is predominantly monoanionic, with the negative charge largely localized on the C_2 oxygen. We suggest that the negative charge on urate at neutral pH gives rise to an inverted orientation in the active site relative to the catalytically productive one for xanthine. This being the case, urate must be considered a poor mimic of substrate in attempting to understand the orientation of the latter in the active site at the outset of catalysis.

In summary, replacing Glu^{232} of *R. capsulatus* xanthine dehydrogenase with glutamine shifts the observed pH profile of k_{red}, consistent with the negatively charged glutamate increasing the pK_a of enzyme-bound substrate by at least two pH units relative to its value in free solution. Further, given the significant (12-fold) decrease in k_{red} associated with the mutation, it is clear that Glu^{232} is in fact ionized and negatively charged in wild-type enzyme. Our results suggest that the ionized Glu^{232}

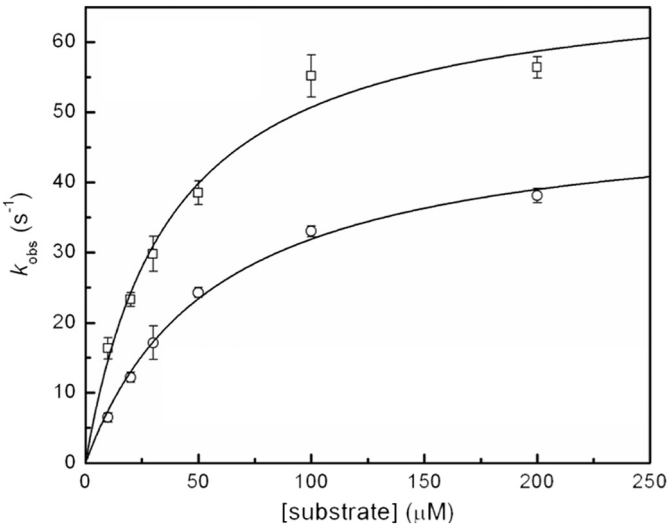

FIGURE 7. **Plots of the observed rate constant k_{obs} *versus* [substrate] for the steady-state reaction of *R. capsulatus* xanthine dehydrogenase with [8-^{1}H]xanthine (*squares*) and [8-^{2}H]xanthine (*circles*).** Uric acid formation was followed at 295 nm at pH 7.8 at 25 °C. k_{cat} and K_m were 69.7 s^{-1} and 37.4 μM with proteated substrate obtained form hyperbolic fits to the data (*solid lines*) and 50.1 s^{-1} and 57.0 μM with deuterated substrate. These yielded deuterium isotope effects on k_{cat} and k_{cat}/K_m of 1.39 and 2.12, respectively.

plays an essential role in substrate specificity, preventing binding of the negatively charged monoanion by electrostatic repulsion. The decrease in k_{red} above pH 7.4 seen here with the E232Q variant observed is consistent the xanthine monoanion now being able to bind in the active site, although it is not acted upon by the enzyme.

Kinetic Isotope Effect Studies of R. capsulatus Xanthine Dehydrogenase—The reductive half-reaction of xanthine consists of two major steps: 1) the initial chemical step of the reaction (nucleophilic attack and hydride transfer to the molybdenum center) that yields product coordianted to the molybdenum center via the catalytically introduced hydroxyl group and 2) product release by displacement of product from the molybdenum center by hydroxide, accompanied by electron transfer out of the molybdenum center. In the wild-type bovine and chicken enzymes, the rate-limiting step has been shown to be product release (12), which is some 75-fold slower than the chemical step of the reaction (24). In light of the significantly larger value k_{cat} and k_{red} seen with wild-type *R. capsulatus* xanthine dehydrogenase relative to the bovine enzyme (30), we have determined the extent to which the chemical step of the reaction is rate-limiting in the bacterial enzyme using a kinetic isotope effect protocol.

Using xanthine deuterated at position 8 as substrate, the apparent primary kinetic isotopic effect on k_{cat} and k_{cat}/K_m ($^Dk_{cat}$ and $^D(V/K)$, respectively) are found to be very small for the bacterial enzyme: 1.39 and 2.12, respectively (Fig. 7). These values are comparable with those seen previously with the bovine and chicken enzymes (24, 29). To determine the intrinsic isotope effect for the chemical step of the reaction, the tritium isotope effect on (V/K) must also be determined, which allows for the subsequent calculation of the extent that the chemical step is rate-limiting. Using a modification of the method of D'Ardenne and Edmondson (24) as detailed under "Experimental Procedures," tritium isotope effect values were

TABLE 4
Kinetic parameters for the steady-state reactions of wild-type *R. capsulatus* xanthine dehydrogenase and the bovine xanthine oxidase

Enzyme	$^D(V/K)$	$^T(V/K)$	^Dk	^DV	fv	k_{cat}	$k_{C\text{-}H}$	k_{off}
						s^{-1}	s^{-1}	s^{-1}
WT XDH	2.12	3.64	5.44	1.39	0.087	69.7	766	76.9
WT XO	1.98	3.62	7.01	1.1	0.016	15	930	15.2

determined for the bacterial xanthine dehydrogenase and, as a control, the bovine oxidase. The results are shown in Table 4, where it can be seen that the tritium isotope effect on (V/K) for the bovine and bacterial enzymes were comparable, at 3.62 and 3.64, respectively. The intrinsic isotope effects calculated as described under "Experimental Procedures" for the bovine and bacterial enzymes are 7.01 and 5.44, respectively, the former value being in acceptable agreement with the previously published value of 7.4 (24). After calculating the fractional velocity (f_v) of the chemical step for each of the enzymes (see "Experimental Procedures"), $k_{C\text{-}H}$ is found to be some ~62-fold faster than k_{cat} for the bovine enzyme and ~12-fold faster for the bacterial enzyme. With the k_{cat} values for each enzyme (Table 3), the rate constant for the chemical step of the reaction for each of the enzymes could be estimated, yielding values of 930 and 766 s^{-1} for the bovine and bacterial enzymes, respectively, which are remarkably similar to one another. Knowing k_{cat} and $k_{C\text{-}H}$ allows calculation of the rate constant for product dissociation, k_{off}, using the following equation.

$$\frac{1}{k_{cat}} = \frac{1}{k_{C\text{-}H}} + \frac{1}{k_{off}} \qquad \text{(Eq. 7)}$$

The values thus obtained are 15.2 and 76.9 s^{-1} for the bovine and bacterial enzymes, respectively. These results demonstrate that the increased rates seen with the bacterial enzyme are due to significantly faster product dissociation rather than acceleration of the chemical step of the reaction.

Unfortunately, the tritium kinetic isotope effects for the E232Q variant (or others, including E730A, E232A, and R310M) could not be reliably determined because of the slow rate of reaction. Even when rates were fast enough to be observed experimentally, consumption of product NADH began to occur (resulting in loss in absorbance at 340 nm) along with a decrease in uric acid (a decrease in absorbance at 295 nm). This does not occur to any significant degree with the wild-type enzyme and could be attributed to reversal of the reaction of bacterial XDH with uric acid and NADH. Given the decrease in the limiting rate of reduction of the variants as compared the wild-type enzyme, the E232A and R310M XDH variants would be expected to exhibit a smaller difference between the rates of the forward and backward reactions, allowing for the reverse reaction to occur much more quickly than the forward reaction after the initial accumulation of uric acid and NADH.

Acknowledgments—We thank Dimitri Niks (Riverside) and Jasmin Kurtzke (Potsdam) for technical assistance.

REFERENCES

1. Hille, R., and Nishino, T. (1995) Flavoprotein structure and mechanism for xanthine-oxidase and xanthine dehydrogenase. *FASEB J.* **9,** 995–1003

2. Hille, R., Nishino, T., and Bittner, F. (2011) Molybdenum enzymes in higher organisms. *Coord. Chem. Rev.* **255,** 1179–1205
3. Enroth, C., Eger, B. T., Okamoto, K., Nishino, T., and Pai, E. F. (2000) Crystal structures of bovine milk xanthine dehydrogenase and xanthine oxidase: Structure-based mechanism of conversion. *Proc. Natl. Acad. Sci. U.S.A.* **97,** 10723–10728
4. Truglio, J. J., Theis, K., Leimkühler, S., Rappa, R., Rajagopalan, K. V., and Kisker, C. (2002) Crystal structures of the active and alloxanthine-inhibited forms of xanthine dehydrogenase from *Rhodobacter capsulatus*. *Structure* **10,** 115–125
5. Huber, R., Hof, P., Duarte, R. O., Moura, J. J., Moura, I., Liu, M. Y., LeGall, J., Hille, R., Archer, M., and Romão, M. J. (1996) A structure-based catalytic mechanism for the xanthine oxidase family of molybdenum enzymes. *Proc. Natl. Acad. Sci. U.S.A.* **93,** 8846–8851
6. Leimkühler, S., Stockert, A. L., Igarashi, K., Nishino, T., and Hille, R. (2004) The role of active site glutamate residues in catalysis of *Rhodobacter capsulatus* xanthine dehydrogenase. *J. Biol. Chem.* **279,** 40437–40444
7. Leimkühler, S., Kern, M., Solomon, P. S., McEwan, A. G., Schwarz, G., Mendel, R. R., and Klipp, W. (1998) Xanthine dehydrogenase from the phototrophic purple bacterium *Rhodobacter capsulatus* is more similar to its eukaryotic counterparts than to prokaryotic molybdenum enzymes. *Mol. Microbiol.* **27,** 853–869
8. Hille, R. (2013) The molybdenum oxotransferases and related enzymes. *Dalton Trans.* **42,** 3029–3042
9. Bray, R. C., Gutteridge, S., Stotter, D. A., and Tanner, S. J. (1979) Mechanism of action of xanthine-oxidase: relationship between the rapid and very rapid molybdenum electron-paramagnetic-resonance signals. *Biochem. J.* **177,** 357–360
10. McWhirter, R. B., and Hille, R. (1991) The reductive half-raction of xanthine-oxidase: identification of spectral intermediates in the hydroxylation of 2-hydroxy-6-methylpurine. *J. Biol. Chem.* **266,** 23724–23731
11. Pauff, J. M., Hemann, C. F., Jünemann, N., Leimkühler, S., and Hille, R. (2007) The role of arginine 310 in catalysis and substrate specificity in xanthine dehydrogenase from *Rhodobacter capsulatus*. *J. Biol. Chem.* **282,** 12785–12790
12. Hille, R. (2005) Molybdenum-containing hydroxylases. *Arch. Biochem. Biophys.* **433,** 107–116
13. Yamaguchi, Y., Matsumura, T., Ichida, K., Okamoto, K., and Nishino, T. (2007) Human xanthine oxidase changes its substrate specificity to aldehyde oxidase type upon mutation of amino acid residues in the active site: roles of active site residues in binding and activation of purine substrate. *J. Biochem.* **141,** 513–524
14. Cao, H., Pauff, J. M., and Hille, R. (2010) Substrate orientation and catalytic specificity in the action of xanthine oxidase: the sequential hydroxylation of hypoxanthine to uric acid. *J. Biol. Chem.* **285,** 28044–28053
15. Ilich, P., and Hille, R. (1997) Tautomerization of the substrate heterocycle in the course of the reaction of xanthine oxidase. *Inorg. Chim. Acta* **263,** 87–93
16. Choi, E.-Y., Stockert, A. L., Leimkühler, S., and Hille, R. (2004) Studies on the mechanism of action of xanthine oxidase. *J. Inorg. Biochem.* **98,** 841–848
17. Pauff, J. M., Cao, H., and Hille, R. (2009) Substrate orientation and catalysis at the molybdenum site in xanthine oxidase: crystal structures in complex with xanthine and lumazine. *J. Biol. Chem.* **284,** 8760–8767
18. Dietzel, U., Kuper, J., Doebbler, J. A., Schulte, A., Truglio, J. J., Leimkühler, S., and Kisker, C. (2009) Mechanism of substrate and inhibitor binding of *Rhodobacter capsulatus* xanthine dehydrogenase. *J. Biol. Chem.* **284,** 8768–8776
19. Okamoto, K., Matsumoto, K., Hille, R., Eger, B. T., Pai, E. F., and Nishino, T. (2004) The crystal structure of xanthine oxidoreductase during catalysis: Implications for reaction mechanism and enzyme inhibition. *Proc. Natl. Acad. Sci. U.S.A.* **101,** 7931–7936
20. Okamoto, K., Kawaguchi, Y., Eger, B. T., Pai, E. F., and Nishino, T. (2010) Crystal structures of urate bound form of xanthine oxidoreductase: substrate orientation and structure of the key reaction intermediate. *J. Am. Chem. Soc.* **132,** 17080–17083
21. Metz, S., and Thiel, W. (2009) A combined QM/MM study on the reductive half-reaction of xanthine oxidase: substrate orientation and mechanism. *J. Am. Chem. Soc.* **131,** 14885–14902
22. Neumann, M., and Leimkühler, S. (2008) Heavy metal ions inhibit molybdoenzyme activity by binding to the dithiolene moiety of molybdopterin in *Escherichia coli*. *FEBS J.* **275,** 5678–5689
23. Kim, J. H., Ryan, M. G., Knaut, H., and Hille, R. (1996) The reductive half-reaction of xanthine oxidase. The involvement of prototropic equilibria in the course of the catalytic sequence. *J. Biol. Chem.* **271,** 6771–6780
24. D'Ardenne, S. C., and Edmondson, D. E. (1990) Kinetic isotope effect studies on milk xanthine oxidase and on chicken liver xanthine dehydrogenase. *Biochemistry* **29,** 9046–9052
25. Simon, H., and Palm, D. (1966) Isotope effects in organic chemistry and biochemistry. *Angew. Chem. Int. Edit.* **5,** 920–933
26. Northrop, D. B. (1975) Steady-state analysis of kinetic isotope-effects in enzymatic reactions. *Biochemistry* **14,** 2644–2651
27. Aguey-Zinsou, K. F., Bernhardt, P. V., and Leimkühler, S. (2003) Protein film voltammetry of *Rhodobacter capsulatus* xanthine dehydrogenase. *J. Am. Chem. Soc.* **125,** 15352–15358
28. Kalimuthu, P., Leimkühler, S., and Bernhardt, P. V. (2011) Xanthine dehydrogenase electrocatalysis: autocatalysis and novel activity. *J. Phys. Chem. B* **115,** 2655–2662
29. Edmondson, D., Ballou, D., Van Heuvelen, A., Palmer, G., and Massey, V. (1973) Kinetic studies on substrate reduction of xanthine-oxidase. *J. Biol. Chem.* **248,** 6135–6144
30. Leimkuhler, S., Hodson, R., George, G. N., and Rajagopalan, K. V. (2003) Recombinant *Rhodobacter capsulatus* xanthine dehydrogenase, a useful model system for the characterization of protein variants leading to xanthinuria I in humans. *J. Biol. Chem.* **278,** 20802–20811
31. Kulikowska, E., Kierdaszuk, B., and Shugar, D. (2004) Xanthine, xanthosine and its nucleotides: solution structures of neutral and ionic forms, and relevance to substrate properties in various enzyme systems and metabolic pathways. *Acta Biochem. Pol.* **51,** 493–531
32. Xia, M., Dempski, R., and Hille, R. (1999) The reductive half-reaction of xanthine oxidase: reaction with aldehyde substrates and identification of the catalytically labile oxygen. *J. Biol. Chem.* **274,** 3323–3330
33. McCrudden, F. H. (1905) *Uric Acid*, Samuel Usher, Boston, MA